Engineering and Technology Journal
Journal homepage: https://etj.uotechnology.edu.iq

An artificial neural network model prediction of mortar strengths reinforced with henequen and sisal fibres for sustainable construction

Akintayo A. Adeniji[a,b]*, Williams K. Kupolati[a], Everardt Burger[a], Mueez Are[b], Jacques Snyman[a], Julius Ndambuki[a], Chris Ackerman[a]

[a] Civil Engineering Dept., Tshwane University of Technology, Pretoria, South Africa.
[b] Civil Engineering Dept., University of Ibadan, Ibadan, Nigeria.
*Corresponding author Email: AdenijiAA1@tut.ac.za

HIGHLIGHTS

- Henequen fibers were extracted from Agave fourcroydes, and sisal fibers were locally sourced.
- Mortar was prepared using a 1:3 cement-to-sand ratio with fibers added in various weight percentages.
- Test samples were cast in cube and prism molds and evaluated for compressive and tensile strength.
- Fiber content had a strong influence on the mechanical performance of the mortar.
- An artificial neural network model was developed to predict the strength properties of the mixes.

Keywords:
Henequen fiber
Sisal fiber
Reinforced mortar
Sustainable construction
Artificial neural network

ABSTRACT

The increasing demand for sustainable building materials has spurred interest in using natural fibers for construction. This study evaluates the performance of henequen and sisal fibers in mortar to enhance their tensile properties and provide alternatives to synthetic fibers. Mortar samples were prepared using a 1:3 mix ratio, with fibers introduced at 0%, 0.5%, 1%, 1.5%, and 2% by weight. The particle size distribution, setting times, consistency, and water ab-sorption and tensile strength of mortar constituents and fibers were determined. Compressive and splitting tensile strength tests were conducted on samples of 75 mm cubes and 50 × 100 mm cylinders at 7, 14, 21, and 28 days, respectively. Data were analyzed using ANOVA at $\alpha = 0.05$ and a validated Artificial Neural Network (ANN) model. Henequen fiber exhibited lower water absorption and higher tensile strength. The 1% mixture recorded the highest com-pressive strength of 15.08 MPa and 15.41 MPa, and the split tensile strength at 0.5% mixture was 3.43 MPa and 3.51 MPa at 28 days, respectively. ANOVA confirmed significant dif-ferences in tensile strength due to fiber inclusion, and compressive strength results indicated no statistically significant differences across samples. The ANN demonstrated high predic-tive accuracy, with R^2 values of 0.8785 and 0.7885, and low mean squared errors of 0.3855 and 0.4855, for compressive and split tensile strengths, supporting its use in performance forecasting. The optimum compressive strength was observed at a 1% fiber content, while the split tensile strength improved up to 0.5%. The experimental results support its application in sustainable construction.

1. Introduction

Mortar is a foundational material in masonry construction, commonly used as a bonding agent in blockwork, plastering, and rendering applications [1,2]. It also enhances structural performance and improves resistance to fire and moisture [3]. Its evolution from lime-based to cement-based mortars reflects advancements in construction technology and growing structural demands [4]. However, conventional cement mortar suffers from low tensile strength and a tendency to crack under stress, limiting its long-term performance in building applications, especially for light structural walls, insulation materials, floor and ceilings, wall coverings, geotextiles, and thatch roofing [5, 6]. To address these limitations and meet the increasing global demand for eco-friendly building materials, researchers have turned to composite and fiber-reinforced mortars with improved mechanical properties [5,7].

The push for sustainable, affordable, and eco-friendly construction has driven interest in modifying mortar compositions [8-10]. Fiber-reinforced mortar not only mitigates cracking but also enhances tensile properties, making it suitable for structural and load distribution in walls, beams, arches, pavements, and interlocking blocks [7]. Both synthetic and natural fibers have been investigated for these purposes [11]. Among natural options, plant-based fibers are increasingly preferred for their renewability, biodegradability, and lower envi-ronmental footprint [12].

http://doi.org/10.30684/etj.2025.161598.1971
Received 17 June 2025; Received in revised form 19 July 2025; Accepted 20 July 2025; Available online 16 August 2025
2412-0758/University of Technology-Iraq, Baghdad, Iraq

Particularly, henequen and sisal fibers extracted from Agave fourcroydes and Agave sisalana, respectively, exhibit high tensile strength, low density, and strong interfacial bonding po-tential when treated appropriately [13,14]. Their integration into mortar contributes to im-proved crack resistance and tensile performance while reducing reliance on synthetic mate-rials and lowering the carbon footprint [15]. These fibers are abundantly available in tropical and subtropical climates, supporting sustainable and cost-effective construction practices [16]. Existing studies have evaluated various fiber types and dosages in mortar systems, including synthetic, recycled, and polymer-based fibers [17-21]. However, limited research has applied predictive modeling to natural fiber-reinforced mortar systems, especially using Artificial Neural Networks (ANN).

This study investigates the mechanical performance and modelling of mortar reinforced with sisal and henequen fibers. The experimental program examines the influence of fiber type, content, and curing age on compressive and split tensile strength. Additionally, characteri-zation tests, including particle size distribution of the sand, cement setting time, and fiber water absorption, were conducted to assess the compatibility of the constituent materials.

To complement the experimental work, an Artificial Neural Network (ANN) model was de-veloped using key input parameters: fiber type, fiber content, and curing age. The model was trained to predict compressive and tensile strength outcomes, with performance evaluated using R^2 and Mean Squared Error (MSE) [22-24]. Traditional empirical models often lack accuracy due to the complex interactions between the components of mortar. ANN provides a data-driven solution to predict performance, optimize mix design, and improve reliability in material selection. The integration of ANN with experimental results strengthens the case for adopting natural fiber reinforced mortar in sustainable construction.

2. Experimental method

2.1 Materials

The henequen fiber used in this study was extracted from Agave fourcroydes using the mechanical and water retting processes, which involve soaking the leaves in water to facilitate the separation of fibers from the surrounding tissue. In contrast, pre-extracted sisal fiber in Figure 1a was sourced for comparative analysis. The binder used was Portland Lime Cement (CEMII/B-L 42.5 N), conforming to the Nigerian Industrial Standard NIS 444-1, ensuring consistent composition and quality. The fine aggregate consisted of sharp sand meeting the grading and cleanliness requirements [25] While the water used in all mortar preparations adhered to World Health Organisation (WHO) standards for potable water, it was used to prevent the introduction of impurities that could affect mortar properties. Figure 1 (b-d) presents visual references, including henequen and sisal plantations, and a horticultural view of the henequen plant, providing context for the origin and characteristics of the fibers utilized in the study.

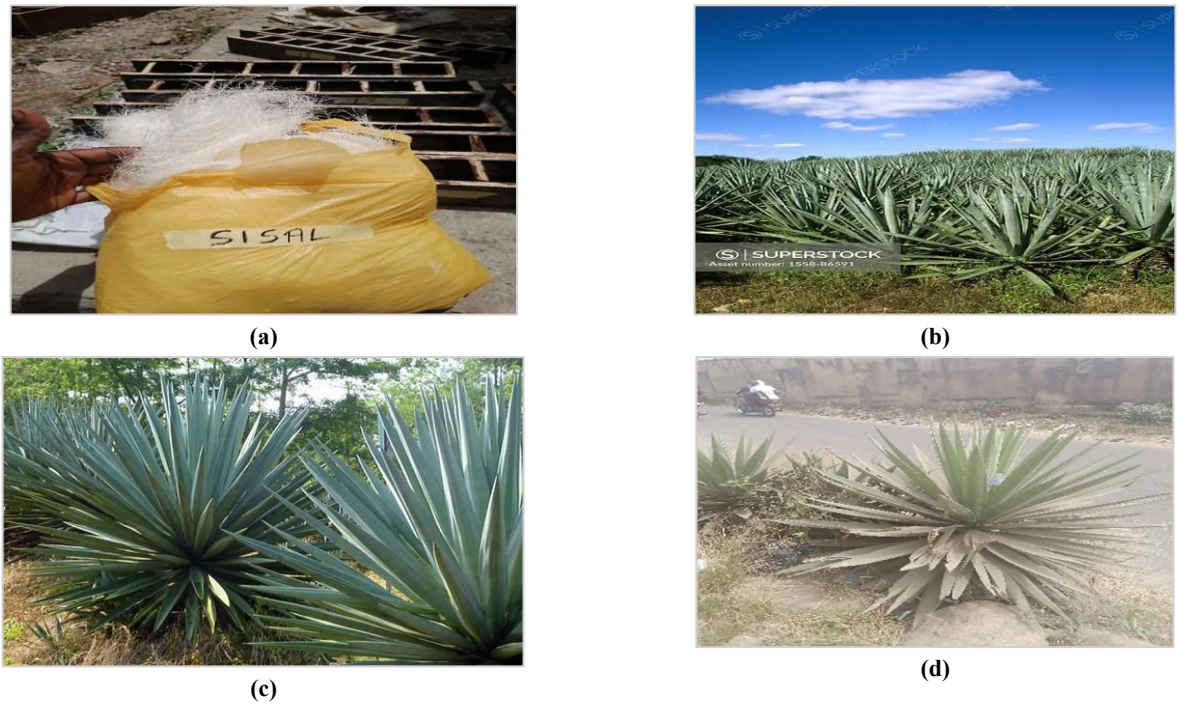

(a) **(b)** **(c)** **(d)**

Figure 1: a) Pre-extracted Sisal Fiber, b) Henequen Plantation (Source: Bisanda and Ansell, 1992), c) Sisal Plantation (Source: Bisanda and Ansell, 1992), d) Henequen Plant as a horticultural plant

2.2 Reinforced mortar samples

2.2.1 Extraction of agave fourcroydes fiber

The extraction of fibers from Agave fourcroydes involves a series of carefully controlled steps to ensure fiber quality and yield [26]. The process begins with the selective harvesting of mature agave leaves using metal blades [27]. Leaves are cut at the base while leaving an adequate portion of the stem intact to allow for plant regrowth. Harvested leaves are then collected and transported in containers to the processing facility [28]. Upon arrival, the leaves were cleaned of dirt and allowed to undergo

decortication, a critical step wherein the fibrous material is separated from the outer layers of the leaf [29]. This is performed manually by scraping the leaves to remove non-fibrous tissue, ensuring minimal waste and maximizing fiber recovery [29]. Following decortication, the extracted fibers are washed to eliminate impurities and plant residues [30]. The fibers are immersed in water tanks and scrubbed with brushes, followed by multiple rinses to ensure complete removal of debris and contaminants [31]. The clean fibers were then air-dried, during which they were carefully arranged to allow uniform airflow and consistent moisture evaporation [32]. Once dried, the fibers undergo brushing and combing to enhance their quality and prepare them for further use. During this step, any loose or entangled fibers are manually removed, and the remaining fibers are aligned and straightened using combs [31]. This process was repeated several times to ensure uniformity in fiber length, thickness, and texture, yielding high-quality natural fibers suitable for reinforcement applications. Figure 2 (a-d) shows the extraction process of fibers from the agave fourcroydes plant.

Figure 2: a) Cleaning of henequen leaves, b) Soaking of henequen leaves, c) Decortication process, d) Extracted henequen fiber, e) Solution of sand sample for Silt content determination, f) Water absorption test on fibers

2.2.2 Properties of sand, cement, and fibers

The sand used for mortar production was evaluated following BS 1199:1976 and BS 1200 standards for building and plastering sands. Sand samples were tested following BS 1377:1990 procedures, particle size distribution, specific gravity, and silt content determination. For particle size distribution, 1000 g of sand was subjected to mechanical sieving using a sieve shaker for 10-15 minutes. The specific gravity in Equation 1 for the sand was determined using a pycnometer through a four-step weighing procedure (W1 to W4), which accounted for dry weight, sample with water, and water-only conditions. Silt content was assessed using Equation 2 by mixing 50 mL of a 1% sodium chloride solution with the sand in a 250 mL cylinder, up to the 150 mL mark, as shown in Figure 2e. After shaking and settling for 3 hours, the volumes of the silt and sand layers were recorded as V1 and V2, respectively, and used to calculate the percentage of silt in the mixture. The initial and final setting times of cement were evaluated using the Vicat apparatus; a 1 mm diameter needle was used to assess the initial setting time, marked by a penetration depth of less than 25 mm. For final setting time, a 5 mm needle was used, with the endpoint determined when the needle no longer visibly penetrated the paste. These tests ensured that materials met the required standards for mortar application. Figure 2f shows the water absorption test for henequen and sisal fibers conducted to evaluate their moisture absorption and retention capacity. The test setup included a precision digital balance for accurate mass measurements, clean water as the

immersion medium, beakers for holding the samples, and a timer to track immersion durations. Figure 2e shows that dried fiber samples, each weighing 5 grams, were individually immersed in separate beakers containing clean water at room temperature. The immersion periods were divided into four 15-minute intervals, totaling one hour, when they were fully saturated. At the end of each interval, the samples were removed, gently blotted to remove surface water without squeezing, and immediately weighed using the digital balance. The percentage of water absorbed was calculated using Equation 3:

$$\text{S.G} = \frac{(W_2 - W_1)}{(W_4 - W_1) - (W_3 - W_2)} \quad (1)$$

$$\text{Silt content} = \frac{V1}{V2}\ X\ 100 \quad (2)$$

$$Water\ Absorption\ \% = \frac{weight\ after\ immersion - weight\ before\ immersion}{weight\ before\ immersion} \times 100\% \quad (3)$$

2.2.3 Mix design proportions of fiber-reinforced mortar samples

The mortar and fiber mix was designed using a mix ratio of 1:3 and a constant water-to-cement (W/C) ratio of 0.6 [33, 34] to ensure adequate workability and hydration. Natural fibers of henequen and sisal were incorporated at 0%, 0.5%, 1.0%, 1.5%, and 2.0% by weight of cement. Fibers were added by weight percentage rather than volume due to their low density and irregular shapes; they occupy more space with less mass, making volume-based measurements unreliable and prone to air gaps and uneven mixing. Weight-based proportioning offers better control relative to cement content, as the cement is measured by weight. Aligning fiber dosage to this unit maintains proportionality and improves result comparability.

These fiber proportions were chosen to evaluate performance limits without compromising mix cohesion or placing difficulties; excessive fiber content can reduce workability. For the compressive strength test, 75 mm × 75 mm × 75 mm cubes were prepared, while 50 mm × 100 mm cylinders were used for the split tensile strength test. Each mix proportion included 20 specimens, and the corresponding material quantities for the compressive strength tests were 2.88 kg of water, 4.80 kg of cement, and 14.42 kg of sand, with fiber contents ranging from 0 to 0.096 kg. For the tensile strength tests, the quantities were 1.33 kg of water, 2.22 kg of cement, and 6.66 kg of sand, with fiber contents ranging from 0.00 to 0.040 kg. Fresh properties of the mixes were assessed by flow and density measurements. Calculations for the quantity of mortar for both compressive and split tensile strength tests are presented below. Table 1(a and b) shows the mix proportions. Figure 3 (a, b, and c) shows the prepared fiber-reinforced mortar samples used in the experimental process.

- Determination of volume of mortar required= =(0.075m x 0.075m x 0.075m)x 20 Nos.= 8.44 x 10^{-3} m^3
- Density of mortar = $\frac{2070kg}{m^3}$
- Weight of 9 cubes of mortar= $\frac{2070kg}{m^3x}$ 8.44 x $10^{-3}m^3$= 17.47 kg
- Allow for 10% wastage= 17.47 kg x 0.1 + 17.47 kg
- Mortar quantity for compressive strength tests = 19.22 kg

Table 1: a) Mix proportions for Compressive Strength Test

Fiber Content (%)	Water (kg)	Cement (kg)	Sand (kg)	Fiber (kg)
0.00	2.88	4.80	14.42	0.00
0.5	2.88	4.80	14.42	0.024
1.00	2.88	4.80	14.42	0.048
1.50	2.88	4.80	14.42	0.072
2.00	2.88	4.80	14.42	0.096

- Determination of volume of mortar required= $\left(\frac{\pi \times 0.05^2 \times 0.1}{4}\right)$ x 20 Nos.= 0.0039 m^3
- Density of mortar= $\frac{2070kg}{m^3}$
- Weight of 9 cubes of mortar= $\frac{2070kg}{m^3x}$ x 0.0039 m^3= 8.073 kg
- Allow for 10% wastage = 8.073 kg x 0.1 + 8.073 kg
- Mortar quantity for split tensile strength tests = 8.88 kg

Table 1: b) Mix proportions for Split Tensile Strength Test

Fiber Content (%)	Water (kg)	Cement (kg)	Sand (kg)	Fiber (kg)
0.00	1.33	2.22	6.66	0.00
0.5	1.33	2.22	6.66	0.11
1.00	1.33	2.22	6.66	0.022
1.50	1.33	2.22	6.66	0.033
2.00	1.33	2.22	6.66	0.040

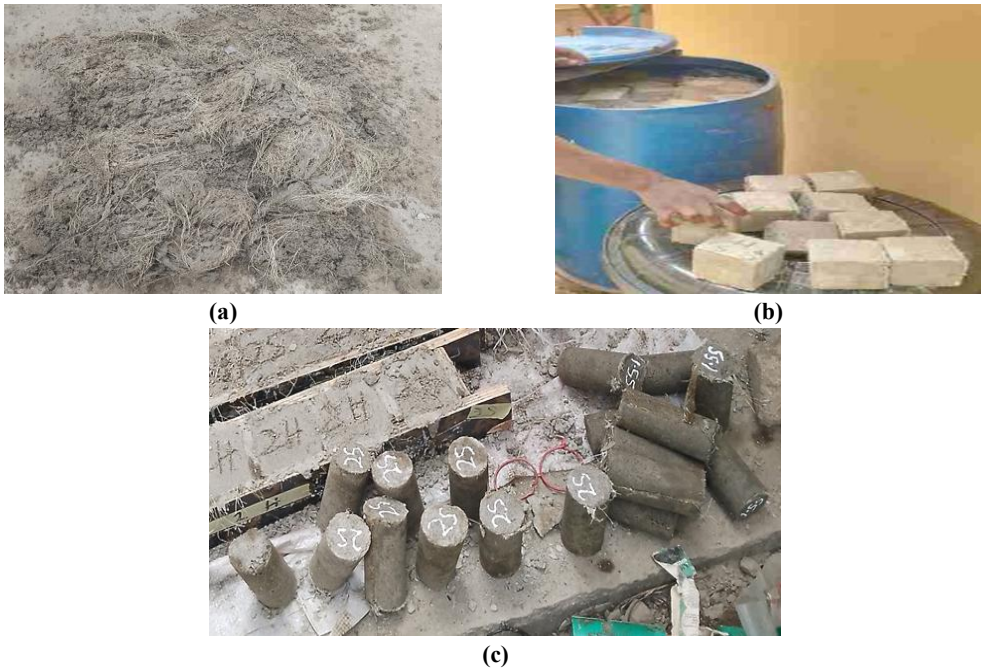

Figure 3: a) Fiber incorporated into fresh mortar sample, b) Cube mortar samples, c) Cylinders mortar samples

2.3 Water absorption test of henequen and sisal fibers

This test provides insight into the hygroscopic behavior of natural fibers. The water absorption test was conducted to evaluate the moisture absorption and retention capacities of henequen and sisal fibers, as these characteristics can significantly influence their mechanical behavior and performance in cement mortar. The apparatus used for the test included a precision digital balance for accurate mass measurement, clean water as the immersion medium, beakers or containers to hold the fibers during immersion, and a timer to control the duration of submersion. For the procedure, dried fiber samples of both henequen and sisal, each weighing 5 grams, were individually immersed in separate beakers filled with clean, room-temperature water. The immersion was carried out in 15-minute intervals over one hour (i.e., at 0, 15, 30, 45, and 60 minutes), at which point a fully saturated condition was observed. At each interval, the fibers were removed from the water, gently blotted to remove surface water without squeezing, and immediately weighed using the digital balance. The percentage of water absorption as per ASTM D 570 [35] was calculated at each interval using Equation 4:

$$Water\ Absorption\ \% = \frac{Wt-Wo}{Wo} \times 100\% \quad (4)$$

where: W_0 = Initial dry weight of the fiber sample (g), W_t = Weight of the fiber sample after immersion at time t (g).

2.4 Tensile strength test of henequen and sisal fibers

Tensile strength is a critical mechanical property of fibers, reflecting their ability to resist breaking under tension. It was tested according to ASTM D2256-10 [36]. It is a fundamental parameter in assessing the suitability of fibers for reinforcement in composite materials, as it directly influences their structural integrity and load-bearing capacity. The tensile strength test was performed on Henequen and Sisal fibers, with three individual samples tested for each fiber type. To ensure consistency, each test specimen was formed by bundling strands of fiber to create a uniform diameter of approximately 1 mm, as verified using a digital Vernier caliper. The ends of the fiber strands were embedded in concrete to ensure a secure grip by the testing machine. The test was conducted using a Universal Testing Machine (UTM), which was calibrated before testing to ensure accuracy in force measurements. Each fiber specimen was mounted securely between the grips of the UTM, ensuring proper alignment and uniform distribution of tension, as shown in Figures 4(a), (b), and (c). The crosshead speed of the UTM was set within the range of 1 to 10 mm/min, following standard testing protocols, depending on fiber type and test conditions such as suitable fiber specimen, length of the specimen should be sufficiently long, at least 1.5 times longer than the gage length, exercise care to avoid fiber twisting, test should be conducted under constant cross-head displacement rate, ensure the machine is calibrated and in equilibrium, and initiating the data recording followed by the operation of the test machine until fiber failure. Before loading, the UTM was zeroed to eliminate any preload on the specimen. The UTM applied a gradually increasing tensile force during the test until the fiber failed. A stress–strain diagram was generated for each sample from which parameters such as tensile strength and tensile modulus could be derived. The maximum tensile load (Fmax) recorded before failure was used to calculate the tensile strength (TS) of each fiber sample, as shown in Equation 5:

$$TS = \frac{F_{max}}{A} \quad (5)$$

where: TS = Tensile strength (MPa), F_{max} = Maximum applied load at failure (kN), A_c = Cross-sectional area of the specimen (mm^2).

(a) (b) (c)

Figure 4: Process of tensile strength test for fiber strand, a) Ends of Fiber, b) Tensile strength test of fibers, and c) Failed sample after strands cast into concrete testing

2.5 Compressive strength test of fiber-reinforced mortar

The compressive strength test was conducted in accordance with BS EN 12390-3:2019 [37] to evaluate the structural performance of mortar reinforced with Henequen and Sisal fibers, specifically assessing the fibers' contribution to enhancing the load-bearing capacity and overall integrity of the mortar matrix. The test was performed [38] using mortar cube specimens cured for 7, 14, 21, and 28 days. After the designated curing periods, the mortar cubes were carefully removed from the curing tank and allowed to acclimate to room temperature. Each specimen was then weighed using a digital weighing balance to document any changes in mass. The Universal Testing Machine (UTM) was used to perform the compressive strength test. Each specimen was centrally aligned on the loading platform of the UTM to ensure concentric loading along its longitudinal axis. A gradual and continuous compressive load was applied at a constant rate until the specimen failed. The UTM continuously monitored and recorded the applied load and deformation throughout the test. The compressive strength (f_c) of each specimen was calculated in Equation 6 by BS EN 12390-3:2019.

$$Compressive\ Strength, f_c = \frac{Fmax}{A_c} \quad (6)$$

where: f_c = Compressive strength (MPa), F_{max} = Maximum applied load at failure (kN), A_c = Cross-sectional area of the specimen (mm^2).

2.6 Split tensile strength test of fiber-reinforced mortar

The split tensile strength test was conducted to evaluate the ability of Henequen and Sisal fibers to enhance the tensile capacity and crack resistance of mortar, which is crucial for assessing their potential as reinforcement in structural applications. This test is particularly effective in measuring tensile strength in brittle materials such as mortar, where direct tension tests are difficult to perform. The test followed the procedures outlined in [38] and was carried out after 7, 14, 21, and 28 days of curing. The apparatus used included a precision weighing balance and a Universal Testing Machine (UTM). Following the curing period, mortar cylindrical specimens (typically 100 mm in length and 50 mm in diameter) were removed from the curing tank and allowed to equilibrate to room temperature. Each specimen was then weighed and carefully positioned horizontally between the platens of the UTM to ensure correct diametral alignment for concentric loading. A compressive load was applied along the diameter of the specimen until failure occurred. This loading induces tensile stress perpendicular to the direction of the applied force, causing the specimen to split along its vertical axis. The split tensile strength (f_{sp}) was calculated using Equation 7, according to BS 116:1983 [39].

$$f_{sp} = \frac{2F_{max}}{\pi DL} \quad (7)$$

where : f_{sp} =split tensile strength (MPa), F_{max}= The maximum load sustained by the specimen (KN), D=specimen diameter (mm), L =length of specimen (mm).

2.7 Artificial neural network (ANN) model

The procedure for applying Artificial Neural Networks (ANN) [40] to predict the compressive and split tensile strength of sisal and henequen fiber-reinforced mortar involves several key stages, each aimed at ensuring accurate and reliable performance modelling [41]. The process begins with data preprocessing, followed by exploratory analysis, correlation examination, and model evaluation [42,43]. Experimental data sets were first collected from laboratory-prepared mortars comprising 400 specimens with the aforementioned mixed proportion of sisal and henequen fibers. Key input parameters include fiber type, dosage, and curing age, while the target outputs are the measured compressive and split tensile strengths at 7, 14, 21, and 28 days. No missing values were observed in the data sets, and the distribution was consistent across all samples and points. The dataset was split into 80% for training (320 samples) and 20% for testing (80 samples) with 14 features after preprocessing. A feedforward ANN architecture is selected for its ability to model non-linear relationships between mix components and mechanical strength [44]. The network consists of an input layer of 14 nodes representing the selected features, two dense layers with 32 units each in the hidden layers, optimized for neuron count and ReLU activation functions, and an output layer that

produces the predicted strength values. The model was trained using forward propagation and backpropagation with gradient descent to minimize prediction errors [45],[41]. Mean squared error is used as the loss function. Model accuracy is validated using metrics such as R^2 and root mean square error. Hyperparameter tuning is performed using Grid Search and K-Fold Cross-Validation (K = 10) to optimize network performance. Once the optimal hyperparameters were determined, the RF model was implemented for predicting compressive and split tensile strength.

3. Results and discussion

3.1 Properties of sand and cement for mortar

Table 2 (a and b) presents the results of the laboratory tests on the sand and cement used in this study. The particle size distribution indicates that less than 35% of the sand passed through the 0.075 mm sieve, confirming its granular nature. Based on the AASHTO classification, the sand falls under category A-2-6, which is a fine aggregate suitable for mortar applications. BS 882:1992 was used to classify the sand sample as Fine sand (F), with a limit of 5 to 70% passing the BS sieve 300 µm. The measured silt content was 4.74%, which is within the permissible limit of 6%, ensuring acceptable purity. The initial and final setting times of the cement were within the specifications of BS 12 for Ordinary Portland Cement. These results meet the recommended standards for mortar production, ensuring that the setting time is neither too rapid nor excessively delayed, as emphasized by the Portland Cement Association (1988) for construction suitability.

Table 2: a) Properties of sand and cement

Properties	Sand
% Passing 0.075 sieve	3.64
% Passing 0.425 sieve	27.05
Specific gravity (g)	2.36
Silt organic content (%)	4.74
AASHTO classification	A-2-6

Table 2: b) Properties of cement

Fineness (%)	3.9
Initial setting time (min)	50
Final setting time (min)	420
Consistency	26.4

3.2 Physical and mechanical properties of fibers

3.2.1 Properties of fibers

The physical and chemical properties of sisal and henequen fibers are presented in Table 3 (a and b) by Muñoz Pérez et al. and Li, Y., and Y.O. Shen [6, 46] reveal characteristics suitable for reinforcing cementitious materials. Both fibers have a length of 75 mm and a diameter of 0.03 mm, with a density of 1.45 g/cm³ and specific gravity of 0.71, conforming to ASTM standards. The fibers exhibit 2.3% elongation at break and a Young's Modulus of 38 GPa, indicating moderate stiffness and tensile capacity. The moisture content was recorded at 12%, indicating a notable level of hygroscopicity. Chemically, the fibers are rich in silicon (18.7%) and aluminum (15.3%), elements known to enhance fiber-matrix bonding and contribute to improved mortar durability.

Table 3: a) Physical properties of sisal and henequen fibers

Description	Results	ASTM Standards
Length (mm)	75	-
Diameter (mm)	0.03	-
Aspect Ratio	0.0004	-
Density (g/cm^3)	1.45	ASTM D3800
Moisture content (%)	12	ASTM D4442
Specific gravity (g/cm^3)	0.71	ASTM C188
Elongation at break (%)	2.3	-
Young's Modulus (GPa)	38	ASTM D3800

Li and Shen [6], Muñoz et al. [46]

Table 3: b) Chemical components of sisal and henequen fibers

Elements	Na	Mg	Al	Si	P	S	K	Ca	Fe
Percentage by mass (%)	12.5	10.8	15.3	18.7	13.2	9.5	8.4	6.3	5.3

Muñoz et al. [46]

3.2.2 Water absorption of henequen and sisal fibers

As illustrated in Table 4 and Figure 5, Sisal fibers exhibited consistently higher water absorption rates than Henequen fibers across all measured time intervals. This observation suggests that Sisal fibers possess a greater affinity for moisture, making them more susceptible to water uptake when compared to Henequen fibers. In contrast, the lower water absorption capacity of Henequen fibers indicates a relative resistance to moisture penetration, which may enhance their dimensional stability and mechanical performance in humid conditions. These differences in hygroscopic behavior have significant implications for the selection of reinforcement materials in mortar and other cementitious composites. Sisal fibers may be more suitable for controlled environments where moisture exposure is limited. In contrast, Henequen fibers are potentially more effective in high-humidity or outdoor applications, where moisture resistance is a critical factor. Further investigation is recommended to assess the long-term effects of environmental conditions, such as temperature fluctuations and wet-dry cycles, on the durability, mechanical integrity, and bonding efficiency of these natural fibers within mortar matrices.

Table 4: Water Absorption

Fiber Sample	Time (minutes)	Weight before immersion (g)	Weight after immersion (g)	Water Absorption (%)
Henequen	15	5	16.4	228
Henequen	30	5	17.9	258
Henequen	45	5	18.1	262
Henequen	60	5	18.5	270
Sisal	15	5	18.7	274
Sisal	30	5	19.8	296
Sisal	45	5	21.1	322
Sisal	60	5	22.2	344

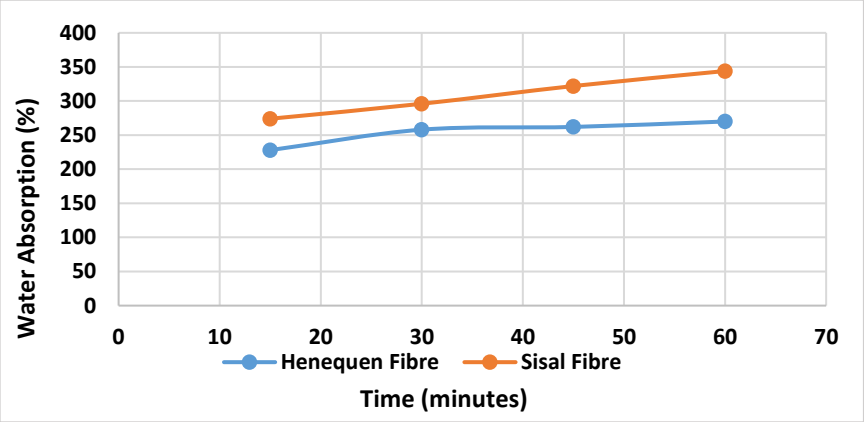

Figure 5: Water Absorption (%) of Henequen and Sisal Fiber

3.3 Tensile strength of fiber samples

Based on the data presented in Table 5, Henequen fibers demonstrated higher tensile strength values compared to Sisal fibers. This result indicates that Henequen fibers possess superior mechanical performance in resisting tensile forces, making them more effective in withstanding stretching or pulling stresses before failure. The enhanced tensile capacity of Henequen fibers suggests their potential suitability for applications that demand greater strength, structural reliability, and long-term durability. Such applications include their use as reinforcement in cementitious composites, where tensile performance plays a crucial role in enhancing crack resistance and structural stability, or in the manufacture of high-performance textiles that require resilience under mechanical loading. These findings contribute to the growing body of knowledge supporting the utilization of plant-based fibers as sustainable alternatives to synthetic reinforcements in construction and other industrial sectors. Compared to Bekele et al. [47], who reported higher tensile strength with 5% NaOH-treated sisal fibers, this study found that untreated sisal and henequen fibers had comparable tensile strengths (~10.7 N/mm²), indicating strong natural performance. Alkali treatment may further enhance these fibers for structural reinforcement applications.

Table 5: Tensile Strength of fiber samples

Fiber Type	Sample Description	Original Length (mm)	Force (N)	Diameter (mm)	Displacement 'ΔL' (mm)	Tensile Strength (N/mm^2)	Average Tensile Strength (N/mm^2)
Sisal	1	400	8.450	1	4.537	10.75887	
	2	400	8.390	1	6.204	10.68248	10.648.52
	3	400	8.250	1	7.312	10.50422	
Henequen	1	400	8.480	1	2.537	10.79707	
	2	400	8.440	1	2.541	10.74614	10.724.92
	3	400	8.350	1	2.553	10.63155	

3.4 Compressive strength of fiber-reinforced mortar

As illustrated in Table 6 (a and b) and Figure 6, the compressive strength results of samples indicated varied performance trends depending on fiber type, content, and curing duration. The control mix demonstrated the highest compressive strength at 28 days, reaching 17.43 MPa, suggesting that the inclusion of fibers does not affect the compressive strength across all mixes. Among the fiber-reinforced samples, 0.5% henequen recorded 15.18 MPa, and 1% sisal with 15.41 MPa exhibited the highest compressive strength at 28 days, followed closely by 1% henequen with 15.08 MPa and 1.5% sisal with 14.49 MPa. This suggests that moderate fiber inclusion, particularly at 0.5 to 1.0%, can maintain or slightly enhance compressive performance relative to higher dosages. All fiber mixes exhibited a progressive strength gain from 7 to 28 days, reflecting the continued hydration and interaction within the fiber matrix. However, 2.0% resulted in reduced strength for both sisal and henequen addition, likely due to poor dispersion, fiber agglomeration, or interference with the matrix continuity. While the presence of fibers may improve other mechanical properties such as crack resistance and ductility, their effect on compressive strength appears to be limited or

even insignificant at higher volumes. The 1% sisal mix exhibited an early strength advantage, reaching 13.48 MPa at 7 days—the highest among all samples at that age, indicating potential for early-age applications. Overall, the results suggest that optimal fiber inclusion lies between 0.5% and 1%, beyond which the benefits diminish. These findings highlight the importance of balancing fiber content to maintain compressive strength while enhancing tensile behavior in sustainable mortar mixtures. Compared to Muñoz et al. and García et al. [46, 48], who reported a 17.80% increase in compressive strength at 1.5% sisal fiber content, the present study observed no statistically significant improvement in compressive strength with fiber addition. While Muñoz Pérez et al. attributed gains to improved fiber dispersion and stress redistribution, this study found reduced compressive performance at higher fiber contents, likely due to clustering and poor matrix integration. However, both studies agree that optimal performance occurs at moderate dosages (0.5–1.5%) and that excessive fiber content (2%) leads to diminished results. Notably, this study found marked improvement in split tensile strength at lower fiber dosages.

Table 6: a) Compressive strength of Fiber-reinforced concrete

Sample	Compressive strength (MPa)			
	7 days	14 days	21 days	28 days
0.5%H	10.52	12.54	14.65	15.18
0.5% S	10.51	11.72	11.78	13.85
1% H	10.58	13.30	13.39	15.08
1% S	13.48	13.73	14.60	15.41
1.5% H	10.56	12.02	12.42	13.32
1.5% S	11.64	12.92	13.71	14.49
2.0% H	10.95	11.84	13.10	13.14
2.0% S	11.89	12.15	12.75	13.08
Control	11.39	14.58	14.91	17.43

Table 6: b) ANOVA Result of compressive strength of mortar samples

	Sum of Squares	Df	Mean Square	F	Sig.
Between Groups	68.037	8	8.505	1.491	.176
Within Groups	410.736	72	5.705		
Total	478.773	80			

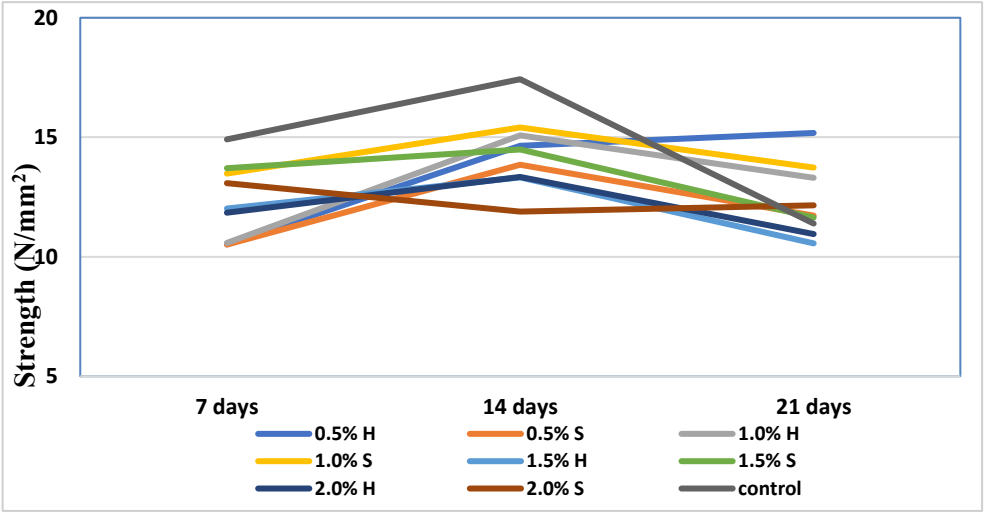

Figure 6: Compressive strength of different Henequen and Sisal fibre-containing mortars samples

3.5 Split tensile strength of fiber-reinforced mortar

The data presented in Table 7 (a and b) and Figure 7 illustrate the split tensile strength of mortar mixtures. The split tensile strength results reveal notable trends in the influence of henequen and sisal fibers on mortar performance over time. The control sample recorded the highest split tensile strength of 3.72 MPa at 28 days; however, some fiber-reinforced mixes approached this value, indicating that fiber inclusion offers competitive tensile performance. Among all the samples, the mix with 0.5% sisal fiber exhibited the highest tensile strength of 3.51 MPa at 28 days, showing a consistent and significant improvement over the other samples. Similarly, the 0.5% henequen fiber mix reached 3.43 MPa, indicating that low fiber dosages are most effective in enhancing tensile properties. This can be attributed to improved fiber matrix bonding and better dispersion at lower concentrations, which enhances crack bridging effects without compromising the integrity of the matrix. In contrast, higher fiber contents, especially 2.0% produced more modest strength gains. The 2.0% sisal and henequen mixes achieved 2.96 MPa and 2.80 MPa, respectively, at 28 days, possibly due to fiber agglomeration and reduced homogeneity, which can introduce voids and weak zones. While the control mix had the highest final strength, samples showed more stable development trends across

curing ages, with moderate but steady increases in strength from 7 to 28 days. The results confirm that fibers are more beneficial to tensile performance than to compressive strength, particularly at contents of 0.5% to 1%. These findings highlight the potential of natural fibers as sustainable reinforcements in mortar, offering improved tensile resistance essential for reducing crack propagation in structural applications while maintaining adequate workability and mechanical integrity. Compared to Muñoz Pérez et al. [46], who reported a 52.3% increase in tensile strength (5.30 MPa) at a 1.5% lime-treated sisal fiber (SF) content, this study recorded a peak of 3.51 MPa at a 0.5% untreated SF content. While both studies confirm enhanced tensile strength at moderate fiber dosages, the lower values in this study may be due to the absence of fiber treatment and shorter fiber length (randomly dispersed 50 mm fibers were used in Muñoz Pérez et al.). Nonetheless, both findings agree that 2% fiber content leads to reduced performance due to fiber agglomeration, poor matrix bonding, and weakened stress distribution efficiency.

Table 7: a) Split tensile strength of fiber reinforced mortar constituents

Sample	Split tensile strength (MPa)			
	7 days	14 days	21 days	28 days
0.5% H	2.83	2.88	3.43	3.43
0.5% S	2.94	3.21	3.36	3.51
1% H	2.77	2.96	2.99	3.00
1% S	2.82	2.95	3.06	3.22
1.5% H	2.31	2.35	2.46	2.71
1.5% S	2.72	2.81	2.85	3.18
2.0% H	2.46	2.60	2.64	2.80
2.0% S	2.75	2.75	2.90	2.96
Control	2.64	3.00	3.30	3.72

Table 7: b) ANOVA Result of split tensile strength of mortar samples

	Sum of Squares	df	Mean Square	F	Sig.
Between Groups	9.578	8	1.197	13.769	.000
Within Groups	6.260	72	.087		
Total	15.838	80			

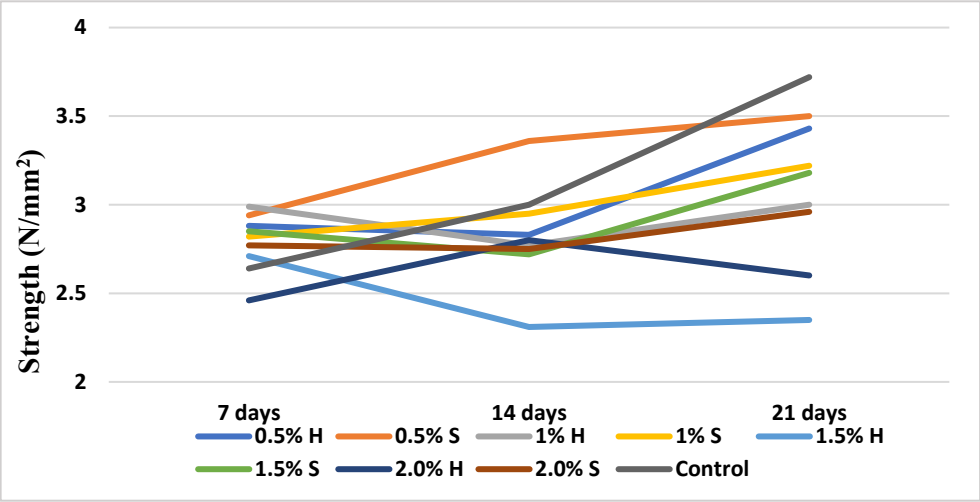

Figure 7: Split Tensile strength of different Henequen and Sisal fibre-containing mortar samples

3.6 Artificial neural network model performance analysis

The ANN model developed for predicting the 28-day compressive and split tensile strengths of sisal and henequen fiber-reinforced mortar demonstrated robust predictive performance, validating its applicability in early-age strength prediction for sustainable construction materials. The model achieved a low mean squared error (MSE) of 0.4855 and 0.3855, a high coefficient of determination (R^2) of 0.7885 and 0.8785%, indicating that approximately 79%, and 88% of the variance in the target variable (28-day compressive and split tensile strength) were successfully explained by the ANN. The result reflects minimal average squared deviation between predicted and observed values, confirming the model's accuracy. A permutation-based feature importance analysis revealed that the 14-day compressive strength was the most influential predictor, followed closely by the 21-day compressive strength. Features representing earlier age results (7-day strength) and categorical inputs, such as sample type (sisal or henequen), also contributed to the model's predictions, but to a comparatively lesser extent. In the same vein, the target variable (split tensile strength) falls within a moderately narrow range, meaning that small absolute errors may result in relatively larger proportional deviations, potentially influencing the model's sensitivity to outliers. This highlights the significance of intermediate-age strength measurements in estimating long-term performance and suggests that mechanical behavior evolves distinctly based on fiber type and matrix interaction. Despite its strengths, the model exhibited signs of slight

underfitting, likely due to variability in the late-age strength values across different fiber compositions and dosages. The incorporation of additional variables—such as concrete mix proportions, water-cement ratio, cement content, and curing conditions—could enhance the model's accuracy and generalizability. Model predictions were presented in Figure 8 (a-d). Figure 8a presents the performance of compressive strength at 28 days, while Figure 8b shows the compressive strength of mortar samples using a boxplot chart where outliers were highlighted. Figures 8c and 8d were the performance and heatmap of the split tensile strength of mortar samples. The ANN approach effectively captured the complex nonlinear relationships between early-age mechanical properties and 28-day strength. The methodology strikes a balance between predictive accuracy and interpretability through deliberate preprocessing, optimal architecture design, and hyperparameter tuning.

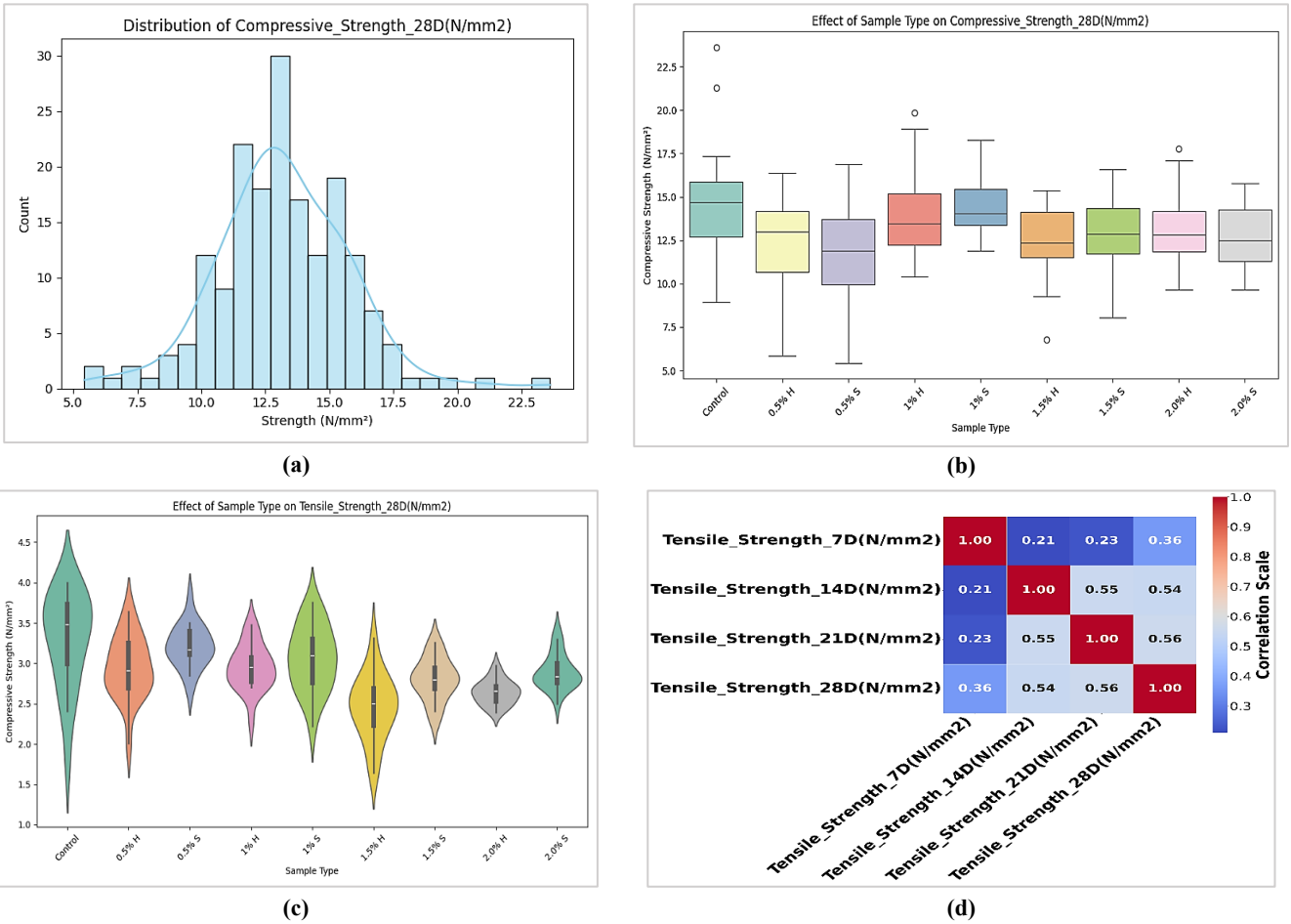

Figure 8: a) Model performance of 28-day compressive strength, b) Artificial neural network performance on the compressive strength c) Artificial neural network performance on the split tensile strength, d) Artificial neural network heatmap of split tensile strength

4. Conclusion

This research evaluated the performance and predictive modelling of henequen and sisal fiber-reinforced mortar using Artificial Neural Networks (ANN) for sustainable construction. Sisal fibers absorbed more water than henequen, suggesting higher moisture susceptibility, while henequen fibers demonstrated superior tensile strength. The compressive strength de-creased slightly with the addition of fiber and showed no statistically significant improve-ment compared to the control. However, split tensile strength improved significantly, espe-cially at 0.5% sisal fiber content, indicating better fiber dispersion and bonding at lower dosages. The ANN model accurately predicted mechanical properties, with high R^2 values and low MSE, validating its use for early performance forecasting. Overall, both fibers ef-fectively enhanced tensile performance without significantly compromising compressive strength, confirming their potential as eco-friendly reinforcements in sustainable mortar applications.

Author contributions

Conceptualization, **A. Adeniji** and **M. Are**; data curation, **A. Adeniji**; formal analysis, **A. Adeniji**; investigation, **A. Adeniji** and **M. Are**; methodology, **E. Burger**; project administration, **W. Kupolati**, resources, **W. Kupolati**.; software, **A. Adeniji**; supervision, **J. Ndambuki** and **J. Snyman**; validation, **W. Kupolati, E. Burger** and **A. Adeniji**; visualization, **C. Ackerman**; writing—original draft preparation, **A. Adeniji**; writing—review and editing, **A. Adeniji**. All authors have read and agreed to the published version of the manuscript.

Funding

This research received no specific grant from any funding agency in the public, commercial, or not-for-profit sectors.

Data availability statement

The original contributions presented in the study are included in the article; further inquiries can be directed to the corresponding author.

Conflicts of interest

The authors declare that there is no conflict of interest.

References

[1] L. G. Baltazar, A. Morais, Assessment of the type of paint on the performance of rendering mortars, CivilEng, 4 (2023) 454-468. https://doi.org/10.3390/civileng4020026

[2] G. Artioli, M. Secco, A. Addis. 2019. The Vitruvian legacy: Mortars and binders before and after the Roman world, Vol. 20, pp. 151–202, published in EMU Notes in Mineralogy. http://dx.doi.org/10.1180/EMU-notes.20.4

[3] M. Caroselli, S. A. Ruffolo, F. Piqué, Mortars and plasters-how to manage mortars and plasters conservation, Archaeol. Anthropol. Sci., 13 (2021) 188. https://doi.org/10.1007/s12520-021-01409-x

[4] W. Yue, B. Wang, Ceramic-added lime and cement mortars: A review of applications in building products, Sci. Prog., 107 (2024). https://doi.org/10.1177/00368504241266559

[5] N. Sathiparan, Performance of sustainable cement mortar containing different types of masonry construction and demolition wastes, Clean Technol. Environ. Policy, 26 (2024) 1861-1881. https://doi.org/10.1007/s10098-023-02681-2

[6] Y. Li, Y.O. Shen, 6-The use of sisal and henequen fibres as reinforcements in composites, Biofiber Reinforcements in Composite Materials, (2015) 165-210. https://doi.org/10.1533/9781782421276.2.165

[7] H. Abdolpour, P. Niewiadomski, A. Kwiecien, M. Tekieli, T. Sadowski, Fundamental understanding of the mechanical and post-cracking behaviour of ultra-high performance mortar with recycled steel fibers. Constr. Build. Mater., 374 (2023) 130918. https://doi.org/10.1016/j.conbuildmat.2023.130918

[8] O. Kirca, Ancient binding materials, mortars and concrete technology: history and durability aspects, Structural Analysis of Historical Constructions; Modena, (2018) 87-95.

[9] P. Cheng, L. Zhang, G. Lin, X. Qian, et al., Effect of different strengthening materials on tensile behaviour of plasters and renders, J. Build. Eng., 56 (2022) 104615. https://doi.org/10.1016/j.jobe.2022.104615

[10] Singh, A., et al., Design for low thermal conductivity and low vibrational impact without efflorescence of the composite bricks developed by waste plastic resin/fly ash/glass powder/gypsum. Int. J. Interact. Des. Manuf., 19 (2025) 949-960. https://doi.org/10.1007/s12008-023-01582-4

[11] J. R. Nayak, J. Bochen, M. Gołaszewska, Experimental studies on the effect of natural and synthetic fibers on properties of fresh and hardened mortar, Constr. Build. Mater., 347 (2022) 128550. https://doi.org/10.1016/j.conbuildmat.2022.128550

[12] Syduzzaman, M., et al., Plant-based natural fibre reinforced composites: a review on fabrication, properties and applications, Coatings, 10 (2020) 973. https://doi.org/10.3390/coatings10100973

[13] Batra, S.K. 1985. Other long vegetable fibers: abaca, banana, sisal, henequen, flax, ramie, hemp, sunn, and coir. Handbook of fiber science and technology, Vol. 4, pp. 727–807.

[14] B. Zuccarello, M. Zingales, Toward high performance renewable agave reinforced biocomposites: Optimization of fiber performance and fiber-matrix adhesion analysis, Composites Part B: Eng., 122 (2017) 109-120. https://doi.org/10.1016/j.compositesb.2017.04.011

[15] R. S. Olivito, O. Cevallos, A. Carrozzini, Development of durable cementitious composites using sisal and flax fabrics for reinforcement of masonry structures, Mater. Des., 57 (2014) 258-268. https://doi.org/10.1016/j.matdes.2013.11.023

[16] M. S. Salit, Tropical natural fibre composites, Tropical Natural fibers and their properties, 15 (2014), http://dx.doi.org/10.1007/978-981-287-155-8

[17] P. Mehrabi, U. Dackermann, R. Siddique, M. Reshidi, A Review on the Effect of Synthetic Fibres, Including Macro Fibres, on the Thermal Behaviour of Fibre-Reinforced Concrete, Buildings, 14 (2024) 4006. https://doi.org/10.3390/buildings14124006

[18] L. A. Oliveira, J.P. Castro-Gomes, Physical and mechanical behaviour of recycled PET fibre reinforced mortar, Constr. Build. Mater., 25 (2011) 1712-1717. https://doi.org/10.1016/j.conbuildmat.2010.11.044

[19] S. M. Raoof, L. N. Koutas, D. A. Bournas, Textile-reinforced mortar (TRM) versus fibre-reinforced polymers (FRP) in flexural strengthening of RC beams, Constr. Build. Mater., 151 (2017) 279-291. https://doi.org/10.1016/j.conbuildmat.2017.05.023

[20] S. MacLennan, F.C. Almeida, A. J. Klemm, The effect of superabsorbent polymers on mechanical characteristics and cracking susceptibility of alkali-activated mortars containing ground granulated blast-furnace slag and copper slag, CivilEng, 3 (2022) 1077-1090. https://doi.org/10.3390/civileng3040061

[21] A. Qorllari, T. A. Bier, Optimization of Workability and Compressive Strength of Self-Compacting Mortar Using Screening Design, CivilEng, 3 (2022) 998-1012. https://doi.org/10.3390/civileng3040056

[22] W. B. Chaabene, M. Flah, M. L. Nehdi, Machine learning prediction of mechanical properties of concrete: Critical review, Constr. Build. Mater., 260 (2020) 119889. https://doi.org/10.1016/j.conbuildmat.2020.119889

[23] M. M. Moein, A. Saradar, K. Rahmati, et al., Predictive models for concrete properties using machine learning and deep learning approaches: A review, J. Build. Eng., 63 (2023) 105444. https://doi.org/10.1016/j.jobe.2022.105444

[24] A. Shaqadan, Prediction of concrete mix strength using random forest model, Int. J. Appl. Eng. Res, 11 (2016) 11024-11029.

[25] S. British, Specification for aggregates from natural sources for concrete. Bs 8821992, 1992.

[26] J. Álvarez-Chávez, M. Villamiel, L. S. Zea, A. K. Jimenez, Agave by-products: An overview of their nutraceutical value, current applications, and processing methods, Polysaccharides, 2 (2021) 720-743. https://doi.org/10.3390/polysaccharides2030044

[27] A. Bismarck, S. Mishra, T. Lampke, Plant fibers as reinforcement for green composites, in Natural fibers, biopolymers, and biocomposites, CRC Press., 52-128, 2005.

[28] M. Brink, R. Escobin, Plant resources of South-East Asia, Backhuys Publ. Leiden, The Netherlands, 17 (2003).

[29] R. Kholiya, A. Goel, Effect of different extraction methods on physical properties of AGAVE species fibers, 2018.

[30] M. A. Mafaesa, Extraction, variability, enzymatic biosoftening and evaluation of physico-mechanical properties of Agave americana L. Fibre, 2020. http://hdl.handle.net/11660/11278

[31] Steyn, H., The evaluation of conventional retting versus solar baking of agave Americana fibres in terms of textile properties, 2006. http://hdl.handle.net/11660/762

[32] J. Patel, P.H. Parsania, Characterization, testing, and reinforcing materials of biodegradable composites, Biodegradable and biocompatible polymer composites: processing, properties and applications, (2017) 55-79. https://doi.org/10.1016/B978-0-08-100970-3.00003-1

[33] B. Standard, BS EN 998-2: specification for mortar for masonry-Masonry mortar, British Standards Institute, 2016.

[34] L. Mollo, Influence of cement/sand ratio on behavior of cement mortar, J. Eng. Design & Technol., 13 (2015) 23-36. http://dx.doi.org/10.1108/JEDT-07-2012-0031

[35] ASTM, Standard test method for water absorption of plastics, ASTM D570-98, Reapproved 2005.

[36] ASTM, Standard Test Method for Tensile Strength and Young's Modulus of Fibers, ASTM C1557-20, 2000.

[37] BSI, Testing hardened concrete: Compressive strength of test specimens, BS EN 12390-3:2019, 2019.

[38] B. Standard, 116 Testing concrete-method for determination of compressive and tensile splitting strength of concrete cubes, British Standards Institute, London, United Kingdom, 1983.

[39] B. Standard, 116 Testing concrete-method for determination of compressive strength of concrete cubes, British Standards Institute, London, United Kingdom, 1983.

[40] D. J. Armaghani, P.G. Asteris, A comparative study of ANN and ANFIS models for the prediction of cement-based mortar materials compressive strength, Neural Comput. Appl., 33 (2021) 4501-4532. https://doi.org/10.1007/s00521-020-05244-4

[41] S. A. Ahmad, H. U. Ahmed, S. K. Rafiq, B. Haddad, Smart predictive modeling for compressive strength in sisal-fiber-reinforced-concrete composites: harnessing SVM, GP, and ANN techniques, Multiscale Sci. Eng., 6 (2024) 95-111. http://dx.doi.org/10.1007/s42493-024-00110-0

[42] B. Joseph, F.H. Wang, S. Shieh, Exploratory data analysis: A comparison of statistical methods with artificial neural networks, Comput. Chem. Eng., 16 (1992) 413-423. http://dx.doi.org/10.1016/0098-1354(92)80057-G

[43] A. Costea, I. Nastac, Assessing the predictive performance of artIficial neural network-based classifiers based on different data preprocessing methods, distributions and training mechanisms, Intell. Syst. Account. Finance Manag. International, J., 13 (2005) 217-250. https://doi.org/10.1002/isaf.269

[44] H. A. Dahish, M. S. Alfawzan, B. A. Tayeh, et al., Effect of inclusion of natural pozzolan and silica fume in cement-based mortars on the compressive strength utilizing artificial neural networks and support vector machine, Case Stud. Constr. Mater., 18 (2023) e02153. https://doi.org/10.1016/j.cscm.2023.e02153

[45] A. Karaci, H. Yapreak, O. Ozkaraca, et al., Estimating the properties of ground-waste-brick mortars using DNN and ANN, Comput. Model. Eng. Sci., 118 (2018) 207-228. https://doi.org/10.31614/cmes.2019.04216

[46] S. P. Muñoz, M. A. Péltroche, E. T. Pachas, et al., Effect of Peruvian sisal fiber on the mechanical and microstructural strength of concrete, Innovative Infrastruct, Solutions, 10 (2025) 257. https://doi.org/10.1007/s41062-025-02061-3

[47] A. E. Bekele, H. G. Lemu, M. G. Jiru, Experimental study of physical, chemical, and mechanical properties of enset and sisal fibers, Polym. Test., 106 (2022) 107453. https://doi.org/10.1016/j.polymertesting.2021.107453

[48] G. García, R. Cabrera, J. Rolon, et al., Natural fibers as reinforcement of mortar and concrete: a systematic review from central and south American regions, J. Build. Eng., 98 (2024) 111267. https://doi.org/10.1016/j.jobe.2024.111267